

# Transactions Letters

## A Novel Receiver Design for Single-Carrier Frequency Domain Equalization in Broadband Wireless Networks with Amplify-and-Forward Relaying

Homa Eghbali, Sami Muhaidat, and Naofal Al-Dhahir

**Abstract**—In this paper, we propose an efficient receiver design for single carrier frequency-domain equalization (SC-FDE) for relay-assisted transmission scenario over frequency selective channels. Building upon our earlier work, we propose a novel minimum mean square error (MMSE)-based receiver design tailored to broadband cooperative networks. We show that, by incorporating linear processing techniques, our MMSE-based receiver is able to collect full antenna and multipath diversity gains, while maintaining low complexity implementation. Specifically, under the assumption of perfect power control and high signal-to-noise ratio (SNR) of the underlying links and assuming either of source-to-relay ( $S \rightarrow R$ ) or relay-to-destination ( $R \rightarrow D$ ) links to be frequency selective Rician fading, our performance analysis demonstrates that the proposed receiver is able to achieve a maximum diversity order of  $\min(L_{SR}, L_{RD}) + L_{SD} + 2$ , where  $L_{SR}$ ,  $L_{RD}$ , and  $L_{SD}$  are the channel memory lengths for  $S \rightarrow R$ ,  $R \rightarrow D$ , and source-to-destination ( $S \rightarrow D$ ) links, respectively. Simulation results demonstrate that our proposed receiver outperforms the conventional cooperative MMSE-SC-FDE receiver by performing close to the matched filter bound (MFB).

**Index Terms**—Single-carrier frequency domain equalization, cooperative diversity, distributed space-time block coding (STBC), equalization, fading channels, pairwise error probability.

### I. INTRODUCTION

THE increasing demand for wireless multimedia and interactive Internet services has led to intensive research efforts on high speed data transmission. A key challenge for high-speed broadband applications is the dispersive nature of frequency-selective fading channels, which causes the so-called intersymbol interference (ISI), leading to an inevitable performance degradation. An efficient approach to mitigate ISI

is the use of single-carrier (SC) modulation combined with frequency domain equalization (FDE). It has been shown that FDE is an attractive equalization scheme for broadband wireless channels which are characterized by their long impulse response memory [1], [2]. Unlike time-domain equalization whose complexity grows exponentially with channel memory and spectral efficiency, SC-FDE enjoys lower complexity, due to its use of the computationally efficient fast Fourier transform (FFT). Furthermore, SC-FDE has several advantages over orthogonal frequency-division multiplexing (OFDM) systems [2], such as large peak-to-average ratio and the sensitivity to carrier-frequency offsets.

Space-time coding has been proposed as a communication technique for wireless system to realize spatial diversity by introducing temporal and spatial correlations into the transmitted signals from different antennas [3]. In [4], Alamouti has proposed an elegant space-time block code (STBC) that guarantees full spatial diversity and full rate over frequency-flat channels. Based on the work of [4], a combination of STBC with SC-FDE for frequency-selective channels presented in [5].

Due to size and power limitations, the deployment of multiple antennas might not be practical for the cellular mobile devices, as well as in ad hoc mobile. Recently, it has been demonstrated that “cooperative diversity” provides an effective means of improving spectral and power efficiency of wireless networks as an alternative to multiple-antenna transmission schemes [6-10]. The main idea behind cooperative diversity is based on the observation that in a wireless environment, the signal transmitted by the source nodes is overheard by other nodes, which can be defined as partners. The source and its partners can jointly process and transmit their information, creating a “virtual antenna array”, although each of them is equipped with only one antenna.

*Related work and contributions:* Although most of the current literature on SC-FDE is limited to point-to-point systems, there have been recent results reported on FDE in the context of cooperative scenarios [6], [11]. Distributed-STBC (D-STBC) SC-FDE has been discussed in [6], assuming the maximum likelihood sequence detector (MLSD) equalization. Although significant diversity gains were demonstrated,

Manuscript received January 20, 2010; revised June 11 and September 8, 2010; accepted November 7, 2010. The associate editor coordinating the review of this letter and approving it for publication was X. Dong.

The work of S. Muhaidat was supported in part by the Natural Sciences and Engineering Research Council (NSERC) of Canada under grant RGPIN372049.

This paper was presented in part at IEEE Globecom 2009, Honolulu, Hawaii, USA, 2009.

H. Eghbali and S. Muhaidat (corresponding author) are with the School of Engineering Science, Simon Fraser University, Burnaby, BC, Canada, V5A 1S6 (e-mail: {hea7@sfu.ca, muhaidat}@ieee.org).

N. Al-Dhahir is with the Dept. of Electrical Engr., The University of Texas at Dallas, Richardson, TX, USA, 75083-0688 (e-mail: aldhahir@utdallas.edu).

Digital Object Identifier 10.1109/TWC.2010.01111.100088

the complexity of the MLSD equalizers increases with the channel memory, signal constellation size, and the number of transmit/receive antennas. This, in turn, places significant additional computational and power consumption loads on the receiver side. Therefore, low-complexity equalization schemes without sacrificing performance are particularly desirable, especially for cases where the receiver implementation is supposed to be simple and required to operate on a limited battery power. In this paper, we propose a novel reduced-complexity MMSE-based receiver design for D-SC-FDE transmissions and demonstrate that our proposed receiver is able to collect full multipath and spatial diversity orders, while providing moderate and low complexity implementation compared to MMSE-D-STBC-SC and MLSD, respectively.

Our contributions in this work are summarized as follows:

- Building upon our earlier work in [12], we propose a novel reduced complexity receiver design for distributed single-carrier frequency domain equalization in a relay-assisted transmission scenario. We assume that either of  $S \rightarrow R$  or  $R \rightarrow D$  links are frequency selective Rician fading.
- We derive the pairwise error probability (PEP) expression for the proposed receiver and show that a maximum diversity order of  $\min(L_{SR}, L_{RD}) + L_{SD} + 2$  is achievable, where  $L_{SR}$ ,  $L_{RD}$ , and  $L_{SD}$  are the channel memory lengths for  $S \rightarrow R$ ,  $R \rightarrow D$ , and  $S \rightarrow D$  links, respectively.
- We present a detailed complexity analysis for the proposed, MMSE-D-STBC-SC, and MLSD receivers.

The rest of this paper is organized as follows: In Sec. II, we describe our assumptions and the relay-assisted transmission model. The reduced-complexity MMSE-based receiver for D-SC-STBC is proposed in Sec. III, followed by the diversity gain analysis in Sec. IV. Computational complexity analysis and numerical results are presented in Sec. V and Sec. VI, respectively. The paper is concluded in Sec. VII.

*Notation:*  $(\bar{\cdot})$ ,  $(\cdot)^T$ , and  $(\cdot)^H$  denote conjugate, transpose, and Hermitian transpose operations, respectively.  $\otimes$  denotes Kronecker product,  $|\cdot|$  denotes the absolute value,  $\|\cdot\|$  denotes the Euclidean norm of a vector,  $[\cdot]_{k,l}$  denotes the  $(k, l)^{th}$  entry of a matrix,  $[\cdot]_k$  denotes the  $k^{th}$  entry of a vector.  $\mathbf{I}_N$  denotes the identity matrix of size  $N$ , and  $\mathbf{0}_{M \times M}$  denotes all-zero matrix of size  $M \times M$ . For a vector  $\mathbf{a} = [a_0 \ \cdots \ a_{N-1}]^T$ ,  $[\mathbf{P}_N^q \mathbf{a}]_s = \mathbf{a}((N-s+q) \bmod N)$  where  $\mathbf{P}_N^q$  is a  $N \times N$  permutation matrix.  $\mathbf{Q}$  represents the  $N \times N$  FFT matrix whose  $(l, k)$  element is given by  $\mathbf{Q}(l, k) = 1/\sqrt{N} \exp(-j2\pi lk/N)$  where  $0 \leq l, k \leq N-1$ . A circularly symmetric complex Gaussian random variable is a random variable  $Z = X + jY \sim \mathcal{CN}(0, \sigma^2)$ , where  $X$  and  $Y$  are i.i.d.  $\mathcal{N}(0, \frac{\sigma^2}{2})$ . Bold upper-case letters denote matrices and bold lower-case letters denote vectors.

## II. SYSTEM MODEL

A single-relay assisted cooperative communication scenario is considered. All terminals are equipped with single transmit and receive antennas. Any linear modulation technique such

as QAM or PSK modulation can be used. We assume amplify-and-forward (AF) relaying and adopt the user cooperation protocol proposed by Nabar *et al.* [13]. Specifically, the source terminal communicates with the relay terminal during the first signaling interval. There is no transmission from source-to-destination within this period. In the second signaling interval, both the relay and source terminals communicate with the destination terminal.

The channel impulse responses (CIRs) for  $S \rightarrow R$ ,  $S \rightarrow D$  and  $R \rightarrow D$  links for the  $j^{th}$  transmission block are given by  $\mathbf{h}_{SR}^j = [h_{SR}^j[0], \dots, h_{SR}^j[L_{SR}]]^T$ ,  $\mathbf{h}_{SD}^j = [h_{SD}^j[0], \dots, h_{SD}^j[L_{SD}]]^T$  and  $\mathbf{h}_{RD}^j = [h_{RD}^j[0], \dots, h_{RD}^j[L_{RD}]]^T$ , respectively, where  $L_{SR}$ ,  $L_{SD}$  and  $L_{RD}$  denote the corresponding channel memory lengths. The  $S \rightarrow R$  link is assumed to be frequency selective Rician fading with power delay profile vector denoted by  $\mathbf{v}_{SR} = [\sigma_{SR}^2(0), \dots, \sigma_{SR}^2(L_{SR})]$  that is normalized such that  $\sum_{l_{SR}=0}^{L_{SR}} \sigma_{SR}^2(l_{SR}) = 1$  [14]. The random vectors  $\mathbf{h}_{RD}^j$  and  $\mathbf{h}_{SD}^j$ , are assumed to be independent zero-mean complex Gaussian with power delay profile vectors denoted by  $\mathbf{v}_{RD} = [\sigma_{RD}^2(0), \dots, \sigma_{RD}^2(L_{RD})]$  and  $\mathbf{v}_{SD} = [\sigma_{SD}^2(0), \dots, \sigma_{SD}^2(L_{SD})]$  that are normalized such that  $\sum_{l_{RD}=0}^{L_{RD}} \sigma_{RD}^2(l_{RD}) = 1$  and  $\sum_{l_{SD}=0}^{L_{SD}} \sigma_{SD}^2(l_{SD}) = 1$ . For the sake of presentation simplicity, the symmetrical scenario, in which the  $R \rightarrow D$  link is considered to be frequency selective Rician fading is omitted here. The CIRs are assumed to be constant over two consecutive blocks and vary independently every two blocks.

Information symbols are first parsed to two streams of  $M \times 1$  blocks  $x_i^j$ ,  $i = 1, 2$  and then multiplied by a zero-padding (ZP) matrix  $\Psi = [\mathbf{I}_M^T, \mathbf{0}_{M \times \ell}^T]^T$  of size  $N \times M$ , where  $\ell = \max(L_{SR}, L_{SD}, L_{RD})$  and  $N$  is the frame length. The use of zero-padding as the precoding method in a single-carrier transmission scenario ensures that the available multipath diversity is fully exploited. To further remove inter-block interference and make the channel matrix circulant, a cyclic prefix (CP) with length  $\ell$  is added between adjacent information blocks. Due to the adopted precoding form, i.e., zero padding, we simply insert additional zeros at the start of the frame as CP. The transmitted blocks for  $S \rightarrow R$  and  $S \rightarrow D$  links are generated by the encoding rule  $\mathbf{d}_1^{k+1} = -\mathbf{J}\mathbf{d}_2^k$ ,  $\mathbf{d}_2^{k+1} = \mathbf{J}\mathbf{d}_1^k$ ,  $k = 0, 2, 4, 6, \dots$ , where  $\mathbf{d}_i = \Psi \mathbf{x}_i$ ,  $i = 1, 2$ , is the zero-padded information vector and  $\mathbf{J} = \mathbf{P}_N^M$  is a  $N \times N$  partial permutation matrix.

## III. MMSE-BASED RECEIVER FOR D-SC-STBC

In this section, we propose a novel, reduced-complexity MMSE-based receiver which enjoys a remarkably simple decoding scheme. We show in the following section that the new proposed receiver is able to collect full antenna and multipath diversity gains.

The proposed receiver includes an MMSE equalizer, followed by linear processing operations. Specifically, the first stage consists of the MMSE-D-STBC-SC scheme [6] with frequency domain equalization, while the second stage is responsible for extracting the underlying multipath diversity by applying linear processing techniques in the time domain.

The signal received at the relay terminal during the first signaling interval is

$$\mathbf{r}_R^j = \sqrt{E_{SR}} \mathbf{H}_{SR}^j \mathbf{d}_1^j + \mathbf{n}_R^j \quad (1)$$

where  $\mathbf{n}_R^j$  is the additive white Gaussian noise vector with each entry having zero-mean and variance of  $N_0/2$  per dimension. The relay terminal normalizes each entry of the received signal  $[\mathbf{r}_R^j]_n$ ,  $n = 1, 2, \dots, N$ , by a factor of  $E \left( |[\mathbf{r}_R^j]_n|^2 \right) = E_{SR} + N_0$  to ensure unit average energy and re-transmits the signal during the second time slot. After some mathematical manipulations, the received signal at the destination terminal in the second time slot is given by

$$\mathbf{r}^j = \sqrt{\frac{E_{RD} E_{SR}}{E_{SR} + N_0}} \mathbf{H}_{RD}^j \mathbf{H}_{SR}^j \mathbf{d}_1^j + \sqrt{E_{SD}} \mathbf{H}_{SD}^j \mathbf{d}_2^j + \tilde{\mathbf{n}}^j. \quad (2)$$

In (2), each entry of the *effective* noise term  $\tilde{\mathbf{n}}_j$  (conditioned on  $\mathbf{h}_{RD}$ ) has zero mean and a variance of  $\rho N_0$  where  $\rho$  is defined by  $\rho = 1 + \frac{E_{RD}}{E_{SR} + N_0} \sum_{m=0}^{L_3} |\mathbf{h}_{RD}(m)|^2$ . In (1)-(2),

$\mathbf{H}_{SR}^j$ ,  $\mathbf{H}_{SD}^j$  and  $\mathbf{H}_{RD}^j$  are  $N \times N$  circulant matrices with entries  $[\mathbf{H}_i^j]_{k,l} = \mathbf{h}_i^j((k-l) \bmod N)$ ,  $i$  denotes  $SR, SD, RD$ , respectively. Finally,  $E_{SR}$ ,  $E_{SD}$  and  $E_{RD}$  are the average energies available at the respective terminal which take into account possibly different path loss and shadowing effects between the  $S \rightarrow D$  and  $R \rightarrow D$  links, respectively. The destination terminal normalizes the received signal by a factor of  $\sqrt{\rho}$ . This does not affect the SNR, but simplifies the ensuing presentation [13]. After normalization, we obtain

$$\mathbf{r}^j = \sqrt{\gamma_1} \mathbf{H}_{RD}^j \mathbf{H}_{SR}^j \mathbf{d}_1^j + \sqrt{\gamma_2} \mathbf{H}_{SD}^j \mathbf{d}_2^j + \mathbf{n}^j \quad (3)$$

where  $\mathbf{n}^j$  is  $\mathcal{CN}(0, N_0)$  and the scaling coefficients  $\gamma_1$ ,  $\gamma_2$  are defined as  $\gamma_1 = \frac{a}{b}$ , and  $\gamma_2 = \frac{c}{b}$  respectively, where  $a = (E_{SR}/N_0)E_{RD}$ ,  $b = 1 + E_{SR}/N_0 + \sum_{m=0}^{L_3} |\mathbf{h}_{RD}(m)|^2 E_{RD}/N_0$ , and  $c = (1 + E_{SR}/N_0)E_{SD}$ . Assuming that the channel coefficients remain constant over two consecutive blocks, i.e.,  $\mathbf{H}_i^k = \mathbf{H}_i^{k+1} = \mathbf{H}_i$ ,  $i$  denotes  $SR, SD, RD$ , the received signals for blocks  $j$  and  $j+1$  are given by

$$\mathbf{r}_1^j = \sqrt{\gamma_1} \mathbf{H}_{RD} \mathbf{H}_{SR} \mathbf{d}_1^j + \sqrt{\gamma_2} \mathbf{H}_{SD} \mathbf{d}_2^j + \mathbf{n}^j \quad (4)$$

$$\mathbf{r}_2^{j+1} = -\sqrt{\gamma_1} \mathbf{H}_{RD} \mathbf{H}_{SR} \mathbf{J} \bar{\mathbf{d}}_2^{j+1} + \sqrt{\gamma_2} \mathbf{H}_{SD} \mathbf{J} \bar{\mathbf{d}}_1^{j+1} + \mathbf{n}^{j+1}. \quad (5)$$

Next, we transform the received signals to the frequency domain by applying the DFT (Discrete Fourier Transform), i.e., multiplying by the  $\mathbf{Q}$  matrix

$$\mathbf{Q} \mathbf{r}^j = \sqrt{\gamma_1} \mathbf{Q} \mathbf{H}_{RD} \mathbf{H}_{SR} \mathbf{d}_1^j + \sqrt{\gamma_2} \mathbf{Q} \mathbf{H}_{SD} \mathbf{d}_2^j + \mathbf{Q} \mathbf{n}^j \quad (6)$$

$$\mathbf{Q} \mathbf{J} \bar{\mathbf{r}}^{j+1} = -\sqrt{\gamma_1} \mathbf{Q} \mathbf{H}_{SR}^H \mathbf{H}_{RD}^H \mathbf{d}_2^j + \sqrt{\gamma_2} \mathbf{Q} \mathbf{H}_{SD}^H \mathbf{d}_1^j + \mathbf{Q} \mathbf{J} \bar{\mathbf{n}}^{j+1}. \quad (7)$$

Exploiting the circulant structure of the channel matrices, we have  $\mathbf{H}_i^j = \mathbf{Q}^H \mathbf{\Lambda}_i^j \mathbf{Q}$ , where  $\mathbf{\Lambda}_i^j$ ,  $i$  denotes  $SR, SD, RD$ , is a diagonal matrix whose  $(n, n)$  element is equal to the  $n^{th}$  DFT coefficient of  $\mathbf{h}_i^j$ . Using the circulant structure and dropping the subscript  $j$  for brevity, we can write (6) and (7) in matrix

form as

$$\begin{aligned} \begin{bmatrix} \mathbf{Q} \mathbf{r}_1 \\ \mathbf{Q} \mathbf{J} \bar{\mathbf{r}}_2 \end{bmatrix} &= \begin{bmatrix} \sqrt{\gamma_1} \mathbf{\Lambda}_{RD} \mathbf{\Lambda}_{SR} & -\sqrt{\gamma_2} \mathbf{\Lambda}_{SD} \\ \sqrt{\gamma_2} \mathbf{\Lambda}_{SD} & -\sqrt{\gamma_1} \mathbf{\Lambda}_{RD} \mathbf{\Lambda}_{SR} \end{bmatrix} \begin{bmatrix} \mathbf{u}_1^k \\ \mathbf{u}_2^k \end{bmatrix} \\ &+ \begin{bmatrix} \mathbf{Q} \mathbf{n}^k \\ \mathbf{Q} \mathbf{J} \bar{\mathbf{n}}^{k+1} \end{bmatrix} = \tilde{\mathbf{\Lambda}} \mathbf{U} + \tilde{\mathbf{N}} \end{aligned} \quad (8)$$

where  $\mathbf{u}_i^j = \mathbf{Q} \mathbf{d}_i^j$  for  $i = 1, 2$  and  $j = k, k+1$ . Since  $\tilde{\mathbf{\Lambda}}$  is an orthogonal matrix of size  $2N \times 2N$ , we can multiply (8) by  $\mathbf{K} = \left( \mathbf{I}_2 \otimes \left( \gamma_1 |\mathbf{\Lambda}_{RD}|^2 |\mathbf{\Lambda}_{SR}|^2 + \gamma_2 |\mathbf{\Lambda}_{SD}|^2 \right)^{-1/2} \right) \tilde{\mathbf{\Lambda}}^H$ . The resulting output streams are now decoupled allowing us to write each output sequence as

$$\mathbf{r}_{out,i}^k = \sqrt{\gamma_1 |\mathbf{\Lambda}_{RD}|^2 |\mathbf{\Lambda}_{SR}|^2 + \gamma_2 |\mathbf{\Lambda}_{SD}|^2} \mathbf{Q} \mathbf{d}_i^k + \mathbf{n}_{out,i}^k \quad (9)$$

where  $\mathbf{n}_{out,i}^k$  is a noise vector with each entry  $\mathcal{CN}(0, N_0)$ . The decoded signal streams in (9) are fed into a minimum Euclidean distance decoder yielding  $\hat{\mathbf{x}}_1$  and  $\hat{\mathbf{x}}_2$ , i.e., a decoded version of the transmitted symbols.

$\hat{\mathbf{x}}_1$  and  $\hat{\mathbf{x}}_2$ , are then fed into the second stage which is capable of exploiting the underlying multipath diversity. Specifically, consider the generation of the matrix  $\mathbf{\Pi}_{i,l}$ ,  $l = 0, 1, 2, \dots, L$ , as follows:

$$\begin{aligned} &[\mathbf{\Pi}_{SRD,l}]_{p,q}, l = 1, \dots, L_{SR} + L_{RD} + 1 \\ &= \begin{cases} 0 & p - q \bmod N = l \\ [\mathbf{H}'_{RD} \mathbf{H}'_{SR}]_{p,q} & p - q \bmod N \neq l, \end{cases} \\ &[\mathbf{\Pi}_{SD,l}]_{p,q}, l = 1, \dots, L_{SD} + 1 \\ &= \begin{cases} 0 & p - q \bmod N = l \\ [\mathbf{H}'_{SD}]_{p,q} & p - q \bmod N \neq l, \end{cases} \\ &[\mathbf{\Pi}_{SD,l}]_{p,q}, l = L_{SD} + 2, \dots, L_{SR} + L_{RD} + 1 = [\mathbf{H}'_{SD}]_{p,q} \end{aligned} \quad (10)$$

where  $1 \leq p, q \leq N$ , then, (4) and (5) can be re-written as

$$\mathbf{y}_1^l = \mathbf{r}_1 - (\sqrt{\gamma_1} \mathbf{\Pi}_{SRD,l} \mathbf{\Psi} \hat{\mathbf{x}}_1 + \sqrt{\gamma_2} \mathbf{\Pi}_{SD,l} \mathbf{\Psi} \hat{\mathbf{x}}_2) \quad (11)$$

$$\mathbf{y}_2^l = \mathbf{r}_2 - (-\sqrt{\gamma_1} \mathbf{\Pi}_{SRD,l} \mathbf{J} \mathbf{\Psi} \hat{\mathbf{x}}_2 + \sqrt{\gamma_2} \mathbf{\Pi}_{SD,l} \mathbf{J} \mathbf{\Psi} \hat{\mathbf{x}}_1). \quad (12)$$

where  $\mathbf{r}_1$  and  $\mathbf{r}_2$  are the received signals in (5) and (6). Under the high SNR assumption which are only to facilitate the analysis [13], we can safely assume that  $\mathbf{x}_1 \approx \hat{\mathbf{x}}_1$  and  $\mathbf{x}_2 \approx \hat{\mathbf{x}}_2$ . Therefore, we can write (11) and (12) as follows:

$$\mathbf{y}_1^l = \sqrt{\gamma_1} \mathbf{H}_{SRD,l} \mathbf{\Psi} \mathbf{x}_1 + \sqrt{\gamma_2} \mathbf{H}_{SD,l} \mathbf{\Psi} \mathbf{x}_2 + \mathbf{n}_1, \quad (13)$$

$$\mathbf{y}_2^l = -\sqrt{\gamma_1} \mathbf{H}_{SRD,l} \mathbf{J} \mathbf{\Psi} \bar{\mathbf{x}}_2 + \sqrt{\gamma_2} \mathbf{H}_{SD,l} \mathbf{J} \mathbf{\Psi} \bar{\mathbf{x}}_1 + \mathbf{n}_2, \quad (14)$$

where  $\mathbf{n}_i$  ( $i=1,2$ ) is  $\mathcal{CN}(0, N_0)$  and

$$\begin{aligned} &[\mathbf{H}_{SRD,l}]_{p,q}, l = 1, \dots, L_{SR} + L_{RD} + 1 \\ &= \begin{cases} [\mathbf{H}_{RD} \mathbf{H}_{SR}]_{p,q} & p - q \bmod N = l \\ 0 & p - q \bmod N \neq l \end{cases} \\ &[\mathbf{H}_{SD,l}]_{p,q}, l = 1, \dots, L_{SD} + 1 = \\ &= \begin{cases} [\mathbf{H}_{SD}]_{p,q} & p - q \bmod N = l \\ 0 & p - q \bmod N \neq l \end{cases} \\ &[\mathbf{H}_{SD,l}]_{p,q}, l = L_{SD} + 2, \dots, L_{SR} + L_{RD} + 1 = 0. \end{aligned} \quad (15)$$

Conjugating  $\mathbf{J} \mathbf{y}_2^l$  and using the fact  $\mathbf{J} \bar{\mathbf{H}}_{i,l} \mathbf{J} = \mathbf{H}_{i,l}^H$ , we obtain

$$\mathbf{J} \bar{\mathbf{y}}_2^l = -\sqrt{\gamma_1} \mathbf{H}_{SRD,l}^H \mathbf{\Psi} \mathbf{x}_2 + \sqrt{\gamma_2} \mathbf{H}_{SD,l}^H \mathbf{\Psi} \mathbf{x}_1 + \mathbf{J} \bar{\mathbf{n}}_2. \quad (16)$$

In matrix form, we can write (13) and (14) as

$$\begin{bmatrix} \mathbf{y}_1^l \\ \mathbf{J}\mathbf{y}_2^l \end{bmatrix} = \underbrace{\begin{bmatrix} \sqrt{\gamma_1}\mathbf{H}_{SRD,l} & \sqrt{\gamma_2}\mathbf{H}_{SD,l} \\ \sqrt{\gamma_2}\mathbf{H}_{SD,l}^H & -\sqrt{\gamma_1}\mathbf{H}_{SRD,l}^H \end{bmatrix}}_{\mathbf{H}_{eq,l}} \begin{bmatrix} \Psi\mathbf{x}_1 \\ \Psi\mathbf{x}_2 \end{bmatrix} + \begin{bmatrix} \mathbf{n}_1 \\ \mathbf{J}\mathbf{n}_2 \end{bmatrix}. \quad (17)$$

After multiplying (17) by  $\left(\mathbf{I}_2 \otimes \left(\gamma_1|\mathbf{H}_{SRD,l}|^2 + \gamma_2|\mathbf{H}_{SD,l}|^2\right)^{-1/2}\right)\mathbf{H}_{eq,l}^H$ , we observe that the output streams are decoupled (due to orthogonality of  $\mathbf{H}_{eq,l}$ ), allowing us to write

$$\mathbf{z}_i^l = \sqrt{\gamma_1|\mathbf{H}_{SRD,l}|^2 + \gamma_2|\mathbf{H}_{SD,l}|^2}\Psi\mathbf{x}_i + \tilde{\mathbf{n}}_i \quad (18)$$

where the noise term is still complex Gaussian with the variance of  $N_0/2$  per dimension. Interestingly, the frequency selective channels are now converted in to parallel independent frequency flat channels. The signals  $\mathbf{z}_i^l, l = 0, 1, \dots, L$ , can now be combined, resulting in

$$\tilde{\mathbf{z}}_i = \sum_{l=0}^L \sqrt{\gamma_1|\mathbf{H}_{SRD,l}|^2 + \gamma_2|\mathbf{H}_{SD,l}|^2}\Psi\mathbf{x}_i + \hat{\mathbf{n}}_i \quad (19)$$

where without loss of generality,  $L = L_{SR} + L_{RD} + 1$  and  $\hat{\mathbf{n}}_i$  is complex Gaussian with variance of  $N'_0 = (L+1)N_0/2$  per dimension. The signals in (19) are then fed into a maximum likelihood decoder to recover the transmitted symbols.

#### IV. DIVERSITY GAIN ANALYSIS

In this section we present the achievable diversity order of the proposed receiver based on the derivation of PEP expression, following [6]. Note that the scheme is different from [6] in the sense that the underlying channel model for either of  $S \rightarrow R$  or  $R \rightarrow D$  links is frequency selective Rician fading. After skipping some steps, which are omitted here due to space limitation, we can write the final PEP expressions as:

**Case I:**  $L_{RD} > L_{SR}$

We found the final PEP expression given as

$$\begin{aligned} P(\mathbf{x}, \hat{\mathbf{x}}) &\leq \frac{(1+n^2)^{L_{SR}+1} e^{-n^2(L_{SR}+1)}}{\binom{L_{RD}+1}{L_{SR}} L_{RD-L_{SR}}} \\ &\times R \left( \frac{E_{SD}}{4N'_0} \right)^{-(L_{SR}+1)} \lambda_{SR}^{-(L_{SR}+1)} \Gamma(L_{RD} - L_{SR}) \quad (20) \\ &\times \prod_{l_{SD}=0}^{L_{SD}} \left( 1 + \frac{E_{SD}}{4N'_0} \lambda_{SD}(l_{SD}) \right)^{-1} \end{aligned}$$

where  $\Gamma[\cdot]$  represents the gamma function [15],  $R = \frac{\binom{L_{RD}+1}{L_{SR}} L_{RD}+1}{\Gamma(L_{RD}+1)}$ , and  $\lambda_{SR}(l_{SR})(\lambda_{SD}(l_{SD}))$  denote the  $l_{SR}^{th}$  ( $l_{SD}^{th}$ ) eigenvalue of codeword difference matrixes between transmitted codeword vector and the erroneously-decoded codeword vector.

**Case II:**  $L_{SR} > L_{RD}$

We found the final PEP expression given as

$$\begin{aligned} P(\mathbf{x}, \hat{\mathbf{x}}) &\leq [(L_{SR} + 1)(L_{SR} + 1 + K_R)]^{L_{RD} - L_{SR}/2} \\ &\times e^{-K_R} \left( \frac{E_{SD}}{4N'_0} \right)^{-(L_{RD}+1)} \prod_{l_{RD}=0}^{L_{RD}} \lambda_{RD}(l_{RD})^{-1} \\ &\sum_{k=0}^{\infty} K_R \frac{\Gamma(L_{SR}+k-L_{RD})}{k!\Gamma(L_{SR}+k+1)} \times \prod_{l_{SD}=0}^{L_{SD}} \left( 1 + \frac{E_{SD}}{4N'_0} \lambda_{SD}(l_{SD}) \right)^{-1} \quad (21) \end{aligned}$$

TABLE I  
COMPARISON OF OVERALL COMPUTATIONAL COMPLEXITY

Implementation	Number of Complex Multiplications
Proposed	$N(\log_2^N + 4) + (N+1)(L_{SR} + L_{SD} + L_{RD} + 2)$
MLSD	$\propto MA^\alpha$
MMSE-D-STBC-SC	$N(\log_2^N + 4)$

where  $K_R = \sum_{l_{SR}=0}^{L_{SR}} K_{l_{SR}}$ , and  $K_{l_{SR}}$  is the Rician parameter on the  $l_{SR}^{th}$  tap. It is observed from (20) and (21) that the maximum achievable diversity order is given by  $\min(L_{SR}, L_{RD}) + L_{SD} + 2$ .

#### V. COMPUTATIONAL COMPLEXITY ANALYSIS

In this section, we focus on the computational complexity of the proposed receiver compared to the MLSD and conventional MMSE-D-STBC-SC receivers. The computational complexity is measured based on the number of the complex multiplications. The overall computational complexity for the proposed, MLSD, and conventional MMSE-D-STBC-SC receivers are summarized in Table I. In the complexity expression for the MLSD receiver,  $M$  is the frame length chosen from an alphabet containing  $A$  complex symbols and  $\alpha = \max(L_{SR} + L_{RD} + 1, L_{SD} + 1)$ .

Fig. 1 illustrates the percentage increase in the computational complexity of the proposed receiver, plotted against the sum of the memory order of the three links,  $L_{SR} + L_{RD} + L_{SD} + 2$ , and  $N$ . For instance, for  $N = 2048$  and  $L_{SR} = L_{RD} = L_{SD} = 1$ , the computational complexity of the proposed receiver is only 33.3% more compared to the conventional MMSE-D-STBC-SC receiver. This percentage is 37.75% for  $N = 1024$  and  $L_{SR} = L_{RD} = L_{SD} = 1$  and 46.69% for  $N = 2048$  and  $L_{SR} + L_{RD} + L_{SD} = 5$ , as illustrated in Fig. 1. Note that even though the implementation of our receiver comes with additional complexity in comparison with the conventional MMSE, it provides a significant improvement in performance in terms of the symbol error rate (SER) performance, which will be illustrated in the numerical results section. This improvement in performance comes at the cost of additional linear processing techniques, which can be implemented easily in practice. It should be further noted that the proposed receiver enjoys a much lower decoding complexity compared to the MLSD receiver, which has certainly prohibitive complexity, specially, when the constellation size of the transmitted signals, channel memory length, and/or the number of participating relays increases. As an example, assuming 4 PSK modulation, for a data block length of  $M = 150$ ,  $N = 1024$ ,  $L_{SR} + L_{RD} + 1 = 4$ , and  $L_{SD} + 1 = 3$ , the MLSD receivers complexity is 78.51% higher than the proposed receiver.

#### VI. NUMERICAL RESULTS

In this section, we present Monte-Carlo simulation results for the proposed receiver, assuming a quasi-static frequency-selective Rician fading channel for the  $S \rightarrow R$  link, which is suitable for suburban areas that a line-of-sight (LOS) path often exists, and quasi-static Rayleigh fading channels for  $S \rightarrow D$  and  $R \rightarrow D$  links. We assume 16-PSK modulation.

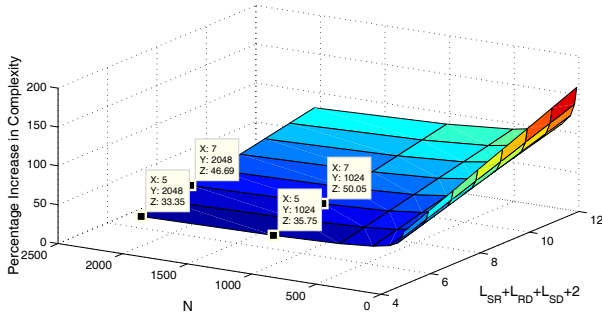


Fig. 1. Percentage increase in the computational complexity of the proposed receiver compared to MMSE-D-SC-STBC.

Rician fading is characterized by the  $K_{l_{SR}}$  factor ( $K_{l_{SR}} = n^2$ ) which is the power ratio of the LOS and the diffused components. It represents Rayleigh fading for  $K_{l_{SR}} = 0$ , and no fading when  $K_{l_{SR}} \rightarrow \infty$ . This makes Rician fading as a general model for land mobile channels [16].

First, the scenarios with different combinations of channel memory lengths are studied. We assume  $E_{SR}/N_0 = 40$  dB and consider three different scenarios. ( $N = 64$ )

- 1)  $L_{SR} = 3, L_{RD} = 2, L_{SD} = 1$  and  $K = 7$  dB
- 2)  $L_{SR} = 3, L_{RD} = 2, L_{SD} = 1$  and  $K = 0$
- 3)  $L_{SR} = 2, L_{RD} = 3, L_{SD} = 1$  and  $K = 0$

In Fig. 2, Performance of MMSE-D-SC-STBC and the proposed receiver for each of these scenarios is illustrated. As a benchmark, we also include MFB performance, which doesn't take ISI into account. It can be seen that identical SER performance is achieved by interchanging the values of  $L_{SR}$  and  $L_{RD}$ , which confirms our previous observations from PEP analysis. It is clear from the slope of the curves that our new receiver is able to collect full diversity gains, i.e.,  $\min(L_{RD}, L_{SR}) + L_{SD} + 2 = 5$ , confirming our earlier conclusion. Our simulation results indicate that, for the first scenario, the proposed receiver outperforms the MMSE-D-SC-STBC equalizer by  $\approx 5.5$  dB at  $SER = 10^{-2}$ . For the second scenario, the proposed receiver outperforms the MMSE-D-SC-STBC receiver by  $\approx 4.5$  dB at  $SER = 10^{-2}$ . The proposed receiver still has a degradation of 1 dB compared to the MFB.

Secondly, we assume  $E_{SR}/N_0 = 40$  dB and consider the following cases in Fig. 3, where performance of the following scenarios is analyzed for MMSE-D-SC-STBC and the proposed receiver. ( $N = 64$ )

- 1)  $L_{SR} = 3, L_{RD} = 1, L_{SD} = 1$  and  $K = 7$  dB
- 2)  $L_{SR} = 3, L_{RD} = 1, L_{SD} = 1$  and  $K = 0$  dB
- 3)  $L_{SR} = 1, L_{RD} = 3, L_{SD} = 1$  and  $K = 0$  dB
- 4)  $L_{SR} = 1, L_{RD} = 3, L_{SD} = 1$  and  $K = 7$  dB

Note that similar SER performance is achieved while interchanging the values of  $L_{SR}$  and  $L_{RD}$ . Our results indicate that for the first scenario, the proposed receiver outperforms the MMSE-D-SC-STBC equalizer by 4.5 dB at  $SER = 10^{-2}$ . Having  $L_{SR} + L_{RD} + L_{SD} + 2 = 7$ , the number of complex multiplications for the proposed receiver is 1095 while the MMSE-D-SC-STBC receiver employs 640 complex multiplication. This extra cost gives  $\approx 4.5$  dB performance increase at  $SER = 10^{-2}$  for the proposed receiver. For the second

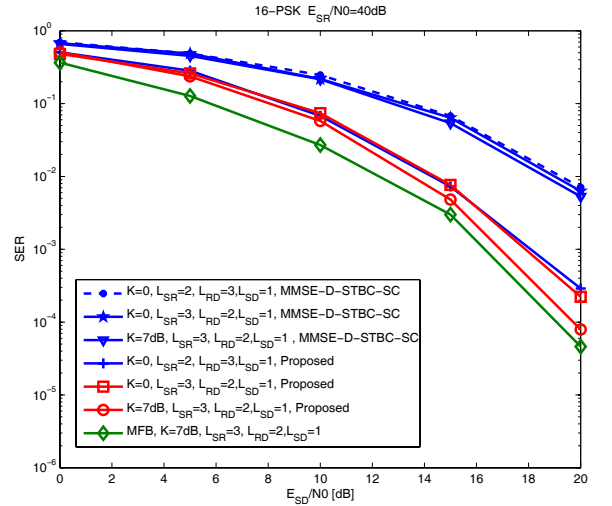


Fig. 2. SER performance of MMSE-D-STBC-SC and proposed receiver.

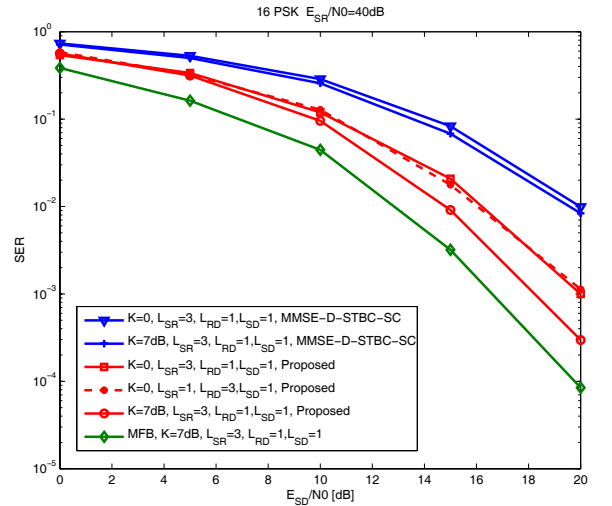


Fig. 3. SER performance of MMSE-D-STBC-SC and proposed receiver.

scenario, the proposed receiver outperforms the MMSE-D-SC-STBC receiver by  $\approx 3$  dB at  $SER = 10^{-2}$ . The proposed receiver has a degradation of 2 dB compared to the MFB.

In Fig. 4, we assume  $L_{SR} = 4, L_{RD} = L_{SD} = 3$ ,  $N = 64$ , and  $K = 7$  dB and study the performance of the system for different  $E_{SR}/N_0$  values. The performance of the proposed receiver degrades as  $E_{SR}/N_0$  decreases, which confirms our earlier observations. It can be seen that at  $SER = 10^{-2}$ , the proposed receiver working at  $E_{SR}/N_0 = 35$  dB outperforms its counterpart working at  $E_{SR}/N_0 = 5$  dB by 15 dB. Interestingly, it is observed from Figs. 2, 3 and 4 that performance improvement of the proposed receiver, in comparison to the benchmark, increases as  $L$  increases, which comes at low additional cost.

In Fig. 5, we plot the performance of the MMSE and proposed receivers for low  $E_{SR}/N_0$  values. We assume 64-PSK. Three scenarios, in conjunction with different combinations of channel memory lengths and different  $E_{SR}/N_0$  values, are considered. ( $N = 64$ )

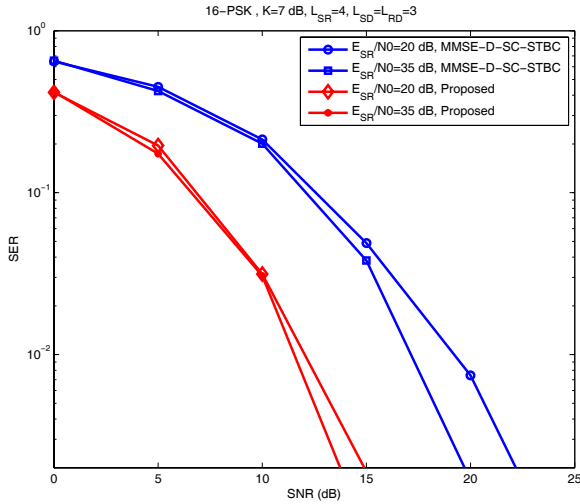


Fig. 4. SER performance of MMSE-D-STBC-SC and proposed receiver.

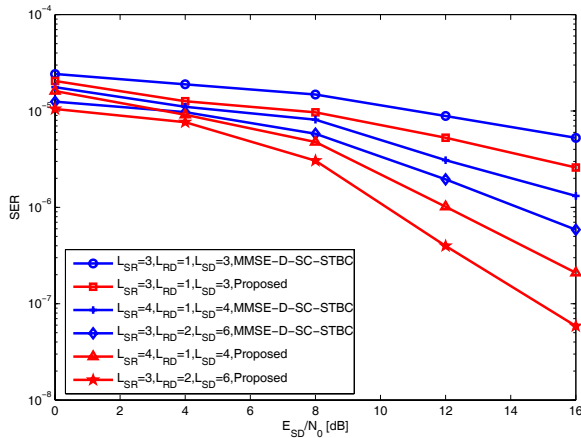


Fig. 5. SER performance of MMSE-D-STBC-SC and proposed receiver.

1)  $L_{SR} = 3, L_{RD} = 1, L_{SD} = 3$ , and  $\frac{E_{SR}}{N_0} = 15$  dB  
 2)  $L_{SR} = 4, L_{RD} = 1, L_{SD} = 4$ , and  $\frac{E_{SR}}{N_0} = 25$  dB  
 3)  $L_{SR} = 3, L_{RD} = 2, L_{SD} = 6$ , and  $\frac{E_{SR}}{N_0} = 25$  dB  
 Simulation results indicate that in the first scenario, where  $E_{SR}/N_0 = 15$  dB, the SER performance of both MMSE-D-SC-STBC and proposed schemes significantly degrades, although the proposed receiver still outperforms the MMSE-D-SC-STBC equalizer, i.e. by  $\sim 4$  dB at  $SER = 10^{-5}$ . For the second scenario where  $E_{SR}/N_0 = 25$  dB, the proposed receiver performs better than the first scenario, by achieving a higher slope. The proposed receiver outperforms MMSE-D-SC-STBC receiver, i.e. by  $\sim 6$  dB at  $SER = 10^{-6}$ . Finally, the SER performance of both schemes is illustrated for the third case where  $E_{SR}/N_0 = 25$  dB and  $L_{SR} = 3, L_{RD} = 2, L_{SD} = 6$ . By collecting higher diversity gains, the proposed receiver achieves the best SER performance of all three scenarios, while outperforming the MMSE receiver i.e. by  $\sim 7$  dB at  $SER = 10^{-6}$ .

In Fig. 6, we show the performance of the proposed receiver and MMSE-D-SC-STBC for large FFT size ( $N = 256$ ) and long channel memory lengths. We assume 64-PSK. Two

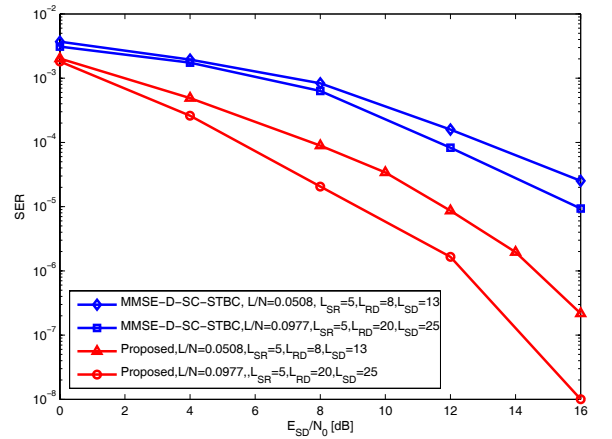


Fig. 6. SER performance of MMSE-D-STBC-SC and proposed receiver.

different scenarios are considered.

- 1)  $L_{SR} = 8, L_{RD} = 5, L_{SD} = 13$  and  $\frac{L}{N} = 0.0508$
- 2)  $L_{SR} = 20, L_{RD} = 5, L_{SD} = 25$  and  $\frac{L}{N} = 0.0977$

It can be seen from Fig. 6 that for the first scenario, where  $L/N = 0.0508$ , the proposed receiver outperforms the MMSE-SC-STBC by  $\sim 6$  dB at  $SER = 10^{-4}$ . For the second scenario, where  $L/N = 0.0977$ , the proposed receiver outperforms the MMSE-SC-STBC by  $\sim 9$  dB at  $SER = 10^{-5}$ . Note that for both scenarios, the complexity of the proposed receiver in terms of complex multiplications compared to the MLSD equalizer is significantly less. However, the proposed receiver incurs moderate computational complexity, three times more for the first scenario, compared to the MMSE-D-SC-STBC equalizer.

## VII. CONCLUSION

We propose a novel reduced-complexity MMSE-based receiver for D-SC-STBC transmissions. We show that, by incorporating linear processing techniques, our MMSE-based receiver is able to collect full antenna and multipath diversity gains, i.e.  $\min(L_{SR}, L_{RD}) + L_{SD} + 2$ . We show that our proposed system incurs moderate and low computational complexity compared to the MMSE-D-STBC-SC and MLSD equalizer, respectively.

## REFERENCES

- [1] M. V. Clark, "Adaptive frequency-domain equalization and diversity combining for broadband wireless communications," *IEEE J. Sel. Areas Commun.*, vol. 16, pp. 1385-1395, Oct. 1998
- [2] H. Sari, G. Karam, and I. Jeanclaude, "Transmission techniques for digital terrestrial TV broadcasting," *IEEE Commun. Mag.*, pp. 100-109, Feb. 1995.
- [3] V. Tarokh, A. Naguib, N. Seshadri, and A. R. Calderbank, "Spacetime codes for wireless communication: combined array processing and space time coding," *IEEE Trans. Inf. Theory.*, vol. 45, pp. 1121-1128, May 1999.
- [4] S. M. Alamouti, "A simple transmit diversity technique for wireless communications," *IEEE J. Sel. Areas Commun.*, vol. 16, pp. 1451-1458, Oct. 1998.
- [5] N. Al-Dhahir, "Single-carrier frequency-domain equalization for space-time block-coded transmissions over frequency-selective fading channels," *IEEE Commun. Lett.*, vol. 5, pp. 304-306, July 2001.

- [6] H. Mheidat, M. Uysal, and N. Al-Dhahir, "Equalization techniques for distributed space-time block codes with amplify-and-forward relaying," *IEEE Trans. Signal Process.*, vol. 55, no. 5, part 1, pp. 1839-1852, May 2007.
- [7] A. Sendonaris, E. Erkip, and B. Aazhang, "User cooperation diversity—part I: system description," *IEEE Trans. Commun.*, vol. 51, no. 11, pp. 1927-1938, Nov. 2003.
- [8] —, "User cooperation diversity—part II: implementation aspects and performance analysis," *IEEE Trans. Commun.*, vol. 51, no. 11, pp. 1939-1948, Nov. 2003.
- [9] J. N. Laneman and G. W. Wornell, "Distributed space-time-coded protocols for exploiting cooperative diversity in wireless networks," *IEEE Trans. Inf. Theory*, vol. 49, no. 10, pp. 2415-2425, Oct. 2003.
- [10] M. Janani, A. Hedayat, T. E. Hunter, and A. Nosratinia, "Coded cooperation in wireless communications: space-time transmission and iterative decoding," *IEEE Trans. Signal Process.*, vol. 52, no. 2, pp. 362-371, Feb. 2004.
- [11] D. Y. Seol, U. K. Kwon, G. H. Im, and E. S. Kim, "Relay-assisted SFBC single carrier transmission over uplink fast fading channels," in *Proc. IEEE Globecom'07*, pp. 3883-3887, Washington, DC, Nov. 2007.
- [12] H. Eghbali, S. Muhaidat, and N. Al-Dhahir, "A low complexity two stage MMSE-based receiver for single-carrier frequency-domain equalization transmissions over frequency-selective channels," in *Proc. IEEE GLOBECOM'09*, Honolulu, HI, Nov. 2009, pp. 1-6.
- [13] R. U. Nabar, H. B'olskei, and F. W. Kneub'uhler, "Fading relay channels: performance limits and space-time signal design," *IEEE J. Sel. Areas Commun.*, vol. 22, no. 6, pp. 1099-1109, Aug. 2004.
- [14] O. Canpolat, M. Uysal, and M. M. Fareed, "Analysis and design of distributed space-time trellis codes with amplify-and-forward relaying," *IEEE Trans. Veh. Technol.*, vol. 56, pp. 1649-1660, July 2007.
- [15] I. S. Gradshteyn and I. M. Ryzhik, *Table of Integrals, Series and Products*. Academic, 2000.
- [16] J. Lu, T. T. Tjhung, F. Adachi, and C. L. Huang, "BER performance of OFDM-MDPSK system in frequency-selective Rician fading with diversity reception," *IEEE Trans. Veh. Technol.*, vol. 49, no. 4, pp. 1216-1225, July 2000.